

Review of thin films of $R\text{Fe}_2\text{O}_4$ ($R=\text{Lu}, \text{Yb}, \text{Tm}$ or In)

Abstract

Rare earth ion ferrite $R\text{Fe}_2\text{O}_4$ ($R = \text{Y}, \text{Dy}, \text{Ho}, \text{Er}, \text{Tm}, \text{Yb}, \text{Lu}, \text{Sc},$ or In) has been attracted much attention due to its anomalous physical properties as a candidate of electronic ferroelectric. Although most of reports were discussed by bulk sample, much effort has been made in fabricating film of $R\text{Fe}_2\text{O}_4$ recently. Finally the charge order was directly observed just recently. Also some data indicate the spin-charge-orbital coupling. In this paper, the film growth and electric, magnetic and optical properties of the films are briefly reviewed.

Keywords: correlated electron system, electronic ferroelectric, film

Volume 2 Issue 2 - 2018

Tomoko Nagata

College of Science and Technology, Nihon University, Japan

Correspondence: Tomoko Nagata, College of Science and Technology, Nihon University, Japan, Tel +81474695457, Email nagata.tomoko@nihon-u.ac.jp

Received: November 17, 2017 | **Published:** March 06, 2018

Introduction

The strongly correlated electron system has been attracted much attention in solid state physics due to its abnormal electric, magnetic and optical properties which promises novel application. Rare earth ion ferrite $R\text{Fe}_2\text{O}_4$ ($R = \text{Y}, \text{Dy}, \text{Ho}, \text{Er}, \text{Tm}, \text{Yb}, \text{Lu}, \text{Sc},$ or In) is the typical example. This material is composed of doubly stacked iron triangular layers (W -layer) separated by single rare-earth triangular layer. Equal amounts of Fe^{2+} and Fe^{3+} exist on triangular lattices and form charge orders due to the Coulombic interaction between iron ions.^{2,3} The charge ordered W -layers stack randomly and regularly above and below three-dimensional charge ordering temperature, respectively.

It has been proposed that each W -layer has microscopic electric spontaneous polarization, and the in-phase and out-of-phase stacking of the polar W -layers generate ferroelectric and antiferroelectric charge orderings respectively.^{4,6} Although the existence of the polar W -layer has been questioned recently,⁷ the macroscopic spontaneous polarization observed by P - E loop supports the existence of the polar W -layer.⁸ These novel ferroelectricity has been called "electronic ferroelectricity",⁹ having great possibility for innovative devices. Since the polarization switching can be realized with only electron hopping and without lattice distortion, low-energy, high-speed and well-repeatable switching is expected. These hypotheses are supported by experimental results. The hopping energy of the electron from Fe^{2+} to Fe^{3+} is confirmed as 0.3 eV by Mossbauer experiments.¹⁰ The charge order can melt and reconstruct in picoseconds order according to the pump probe experiments.¹¹ Furthermore, the melting of the charge order provokes non-linear electric conductivity which can be used as a switching device.¹²

$R\text{Fe}_2\text{O}_4$ also shows interesting magnetic property. Each W -layer also has the net magnetic moment due to the ordering of the spins on iron ions.¹³ The two kinds of stacking manner of the magnetic W -layers generate ferrimagnetism and antiferromagnetism in analogy with ferroelectricity and antiferroelectricity. Since both of the electric and magnetic properties arise from the ordering of iron ions, correlation is expected between electric and magnetic properties. Actually we have reported a magnetoelectric effect.¹⁴

Most of these attractive properties were observed in bulk sample. The key for the application of $R\text{Fe}_2\text{O}_4$ is the film growth. However, the film fabrication of this material is still a developing research due to the difficulty in selecting substrates and keeping the stoichiometry, which changes various properties significantly.^{15,16} 13 reports have been published by 2017,¹⁷⁻²⁹ following the first report by M. Seki et al in 2010.¹⁷ In this paper, the film growth and electric, magnetic and optical properties of the films are briefly reviewed.

Fabrication of the film

Various trivalent ions are selected as R ion in reported films: Lu ,¹⁸⁻²⁵ Yb ,²⁶⁻²⁸ Tm ¹⁷ and In .²⁹ The change in R ions is unlikely to affect intrinsically as well as for bulk. These films are fabricated on various substrates: $\text{Al}_2\text{O}_3(001)$,^{18,21,25,26,28}

$\text{YSZ}(111)$,^{17,19,24,27} $\text{ZnO}(001)$,²⁹ $\text{MgO}(111)$,^{20,22,23} $\text{MgAl}_2\text{O}_4(111)$ ²³ and $6\text{H-SiC}(001)$.²³ Although the lattice mismatch is not small with all substrates, MgAl_2O_4 is likely to have the best lattice constant in these substrates. Clean interface is observed on MgAl_2O_4 substrate with MgAl_2O_4 [2-1-1]// LuFe_2O_4 [100] without any impurity and disordered layers as shown in Figure 1.²³

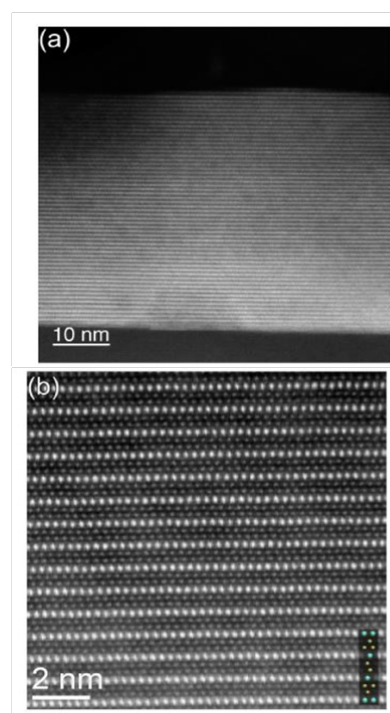


Figure 1 High angle annular dark field scanning transmission electron microscopy images of the LuFe_2O_4 film on MgAl_2O_4 substrate showing (a) the presence of a clean interface and (b) the well-ordered structure of $\text{LuO}_{1.5}$ layers alternating with $\text{Fe}_2\text{O}_{2.5}$ layers. An overlay of a single unit cell is shown in the lower corner of (b).²³

Also various deposition techniques are tried: pulsed laser deposition (PLD),^{17,18,20,21,24,27,29} electron beam deposition (EB),^{19, 25,26} molecular beam epitaxy (MBE),^{22,23} and rf magnetron sputtering.²⁸ The most popular way to fabricate $R\text{Fe}_2\text{O}_4$ film is PLD. The ablation is performed on $R\text{Fe}_{2-x}\text{O}_{4+y}$ target prepared by solid state reaction. The chamber pressure during the deposition differs depending on the groups; 10^{-5} Pa ~ 1 Pa. Although most of all substrates are heated up to 700°C ~ 900°C , too much heating often lead iron defects.²⁷

The as-depo films are annealed in some reports.^{17,21,24} Although each group tried optimization of the deposition condition and discussed the composition, crystal structure and morphology, the conclusion differs depending on the groups. EB realizes higher crystallized film, despite of poor orientation. $R\text{Fe}_{2-x}\text{O}_{4+y}$ target is prepared by solid state reaction. The chamber pressure and substrate temperature are almost the same as those of PLD. As for MBE, iron and rare earth elemental fluxes are provided from different effusion cells. The deposition condition is simulated by calculation.²³

In these various deposition techniques, much effort has been made to get high stoichiometric film.^{18,21,23,27,28} The most popular way to overcome easier vaporization of Fe is deposition in Fe-rich environment: Fe enriched target or higher power of Fe source. Kashimoto R et al.²⁷ suppressed revaporization of Fe ion by detail investigation of the emission intensity variation of each element with defocus degree, chamber pressure and substrate temperature.²⁷ The substitution of Cu for a half amount of Fe is also effective to control the ratio of divalent ions to trivalent ions because Cu^{2+} and Fe^{3+} are stable.¹⁷ However, Fe-rich environment often generates Fe_3O_4 in initial growth.

Fujii T et al.²⁸ utilized Fe_3O_4 as a buffer layer and succeeded in getting the highest crystallization by rf magnetron sputtering.²⁸ The Fe_3O_4 was deposited on Al_2O_3 (0001) substrate at first, and then YbFe_2O_4 was fabricated on the Fe_3O_4 layer. They prepared two cathodes; one for pure Fe target and another for Yb_2O_3 target. The powers of the two cathodes were controlled separately. Figure 2 shows cross section transmission electron microscopy (TEM) image of the bilayer film and selected area electron diffraction (SAED). Clear superlattice diffraction spots are observed in the panel C, indicating the formation of the charge order with long coherence length. This is the only one report of the crystal in which the existence of the charge order is confirmed at present.

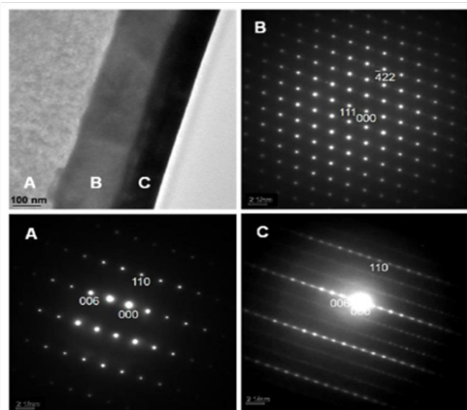


Figure 2 Cross section TEM image of the YbFe_2O_4 film on Al_2O_3 (0001) substrate with Fe_3O_4 buffer layer. SAED patterns taken from the substrate (A), Fe_3O_4 buffer layer (B) and YbFe_2O_4 film layer (C) are also provided.²⁸

Magnetic property

The intrinsic magnetic property is likely to be the same as that of bulk as reported in refs.^{20,23,28} Figure 3 shows the magnetization as a function of temperature and magnetic field.²³ The most of the $M-H$ loop of the film show similar curve with Figure 3. Both of film and bulk samples often show hysteresis and large coercive field and saturation magnetization. The single and double hysteresis loops are observed in stoichiometric and off-stoichiometric samples, respectively.³⁰ The peak in zero field cooling (ZFC) curve also indicates high stoichiometry.³⁰ As for Figure 3, the relatively high stoichiometry of the film on SiC substrate is indicated by the peak in ZFC curve and near single hysteresis loop in $M-H$ curve.^{23,30} The Neel temperature (T_N) is a little lower than that of the bulk, which likely to arise from lower crystallization or longer c -axis and shorter a - and b -axes by stress from the substrate. The coercive field is small in refs.^{26,29} due to size effect.

Seki M et al.²⁹ reports magnetic memory effect.¹⁷ The memory in the cooling process is read in the heating process. The sample was cooled under the magnetic field from 200K to 4K with a pose at 10K. Then the magnetization

showed clear jump at 10 K in the heating process as shown in Figure 4. Such memory effect is a step in research for application.

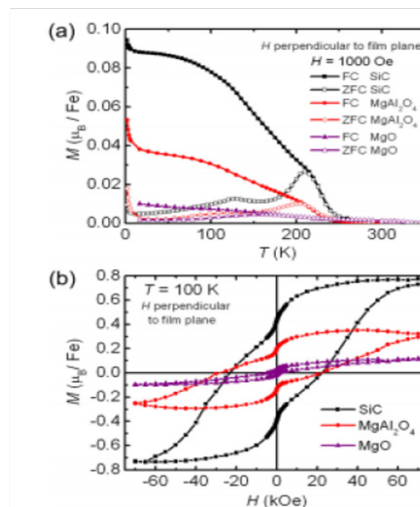


Figure 3 The magnetization as a function of temperature (a) and magnetic field (b) of LuFe_2O_4 films on SiC, MgAl_2O_4 and MgO substrates.²³

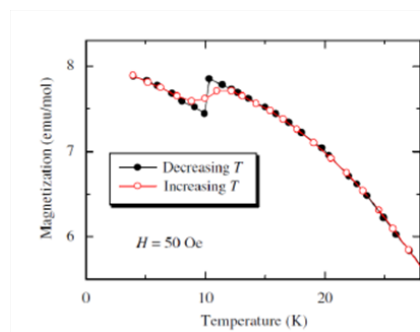


Figure 4 Temperature dependence of magnetization for the TmFeCuO_4 thin film. The solid black circles are measured during cooling in 50 Oe at a constant rate of 4K/min with a stop of 4h duration at 10K. The field was switched off during a stop. The open red circles are measured with continuous heating at the same rate after the previous cooling procedure.¹⁷

Electric property

The electric property is reported in refs.^{18-19, 21, 24-28} The intrinsic electric property is also likely to be the same as that of bulk. The resistivity significantly differs depending on the stoichiometry. $1 \Omega\text{cm} \sim 104 \Omega\text{cm}$ of the resistivity is reported at room temperature. The higher resistivity indicates higher stoichiometry. As for the temperature dependence, the electric property shows anomaly around T_N and three-dimensional charge-ordering temperature, T_{CO} .^{21,24,26} Figure 5 shows the temperature dependence of resistance of the film.²¹ The discontinuous change and kink are observed at T_{CO} and T_N in $R-T$ curve respectively. The same sample shows significant peak at T_{CO} in the loss term of dielectric constant. However the magnitude of the anomalies depends on the sample. The sample in ref.²⁶ shows anomaly only at T_N in $R-T$ curve. The sample in ref.²⁴ shows anomaly only at T_{CO} . Aside from the magnitude, these anomalies at T_{CO} and T_N indicate spin-charge coupling and the charge order as the key of the electric property. Although such anomalies are reported also in bulk, films show larger anomalies. It is important that the spin-charge coupling become prominent in film rather than be kept.

The dielectric property is reported in refs.^{18,21} The large dielectric constant is observed with gold electrodes while the intrinsic dielectric constant is small in bulk. The larger dielectric constant of the film may arise from high conductivity or off-stoichiometry which changes fermi level.³¹ Accompanied

by the change in the magnitude of the interface effect between the sample and gold electrodes. The dielectric tunability is also reported.^{18,21} Figure 6 shows the dielectric tunability of the film under the electric field and magnetic field.²¹ The dielectric constant decreases 35% under 5kV external electric field. Furthermore, the dielectric tunability can be changed by external magnetic field. These results also indicate the spin-charge coupling and great possibility for application.

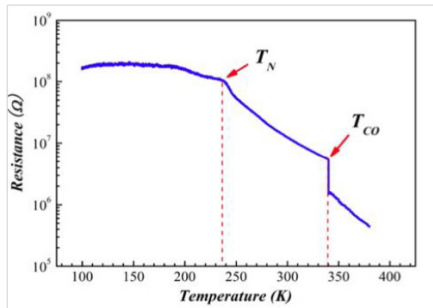


Figure 5 Temperature dependence of resistance of LuFe_2O_4 film during heating.²¹

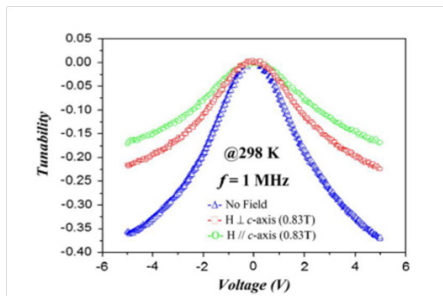


Figure 6 Dielectric tunability of the LuFe_2O_4 film measured at room temperature under the electric field and the magnetic field.²¹

Huge nonlinear electric conductivity is reported in ref.²⁴ Both of the intrinsic nonlinearity¹² and Jule effect are likely to be detected. The nonlinear electric conductivity can be observed significantly in the film since the thin film can be applied much larger electric field than bulk. Hall effect is also reported.²⁵ The p - and i -type conductivity are observed above and below 440K, respectively, indicating the film keeps the bulk property.

Optical property

The films have advantage in research on the optical property than bulk. The optical property is reported in refs.^{19, 23, 25-26} Figure 7 shows representative absorption spectra of LuFe_2O_4 film as a function of photon energy at 78 and 300K.¹⁹ The peaks are observed around 1.6 eV, 2.4 eV and 3.3 eV, corresponding to the Fe^{2+} d to d on-site transition and the $\text{O } 2p$ to $\text{Fe } 3d$ charge-transfer transition, estimated from first-principles electronic structure calculations.³² The band gap was estimated to 0.3 eV and 2.4-3.4 eV as indirect and direct gaps, respectively. The temperature dependence of the spectra is also discussed. The direct band gap become larger with decreasing temperature.^{19,26} The significant anomaly is observed in the band gap around T_{CO} and T_N .¹⁹ Moreover, the absorption spectra of the charge transfer show sharp decline at T_N . Also clear differences are reported in optical spectra between below and above T_{CO} in ref.²⁶ These results indicate strong spin-charge-orbital coupling. The anomaly is also observed around 180K, suggesting the structure distortion²⁶ while the physics around 180K has been controversial topic in bulk.

Furthermore, refs.^{25,26} reported electro-optical effects. 9% of large electro-optical effects are reported under 500 V/cm of the electric field at 10K.²⁶ The magnitude of the electro-optical effect increases with decreasing the temperature.²⁵ Figure 8 shows the electro-optic signal at 78 and 170K.²⁵ The electro-optical effects are +4% ~ -5% at 78K, and +3.5 ~ -1.5% at 170K under 200 V/cm of the electric field. Above T_N , they observed very small (<1%) electro-optical effects. The large electro-optical effects below T_N indicates a

strong spin-charge coupling. The inset of Figure 8 shows the largest electro-optical signal as a function of applied voltage at 78K and 170K. Linear electro-optical effects are observed. The mechanism of the electro-optical effect in this material may be different from that in the perovskite-type ferroelectrics since the mechanism of the ferroelectricity is likely to be different. The research on the optical property will be more progressed by recent higher quality films.

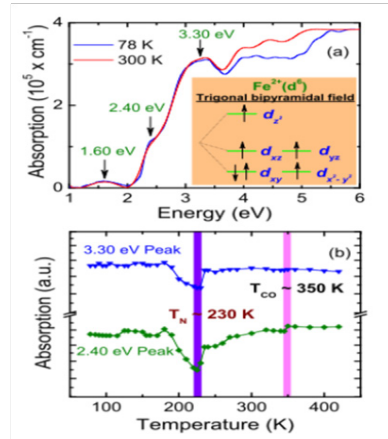


Figure 7 Representative absorption spectra of the LuFe_2O_4 film on sapphire at 78 and 300K, extracted from the transmittance data. The arrows indicate the electronic transitions. The inset shows the Fe^{2+} (d^6) crystal-field splitting scheme. (b) The absorption peaks at 2.40 eV (Fe^{2+} d to d on-site) and 3.30 eV ($\text{O } 2p$ to $\text{Fe } 3d$ charge transfer) transitions as a function of temperature. The shaded vertical lines designate T_N and T_{CO} .¹⁹

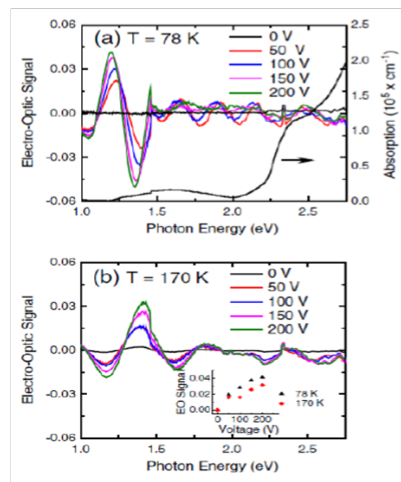


Figure 8 Electro-optical effects in applied dc voltages up to 200V, and the absorption coefficient of the LFO thin film in the photon energy range of 1–2.75 eV at (a) 78K and (b) 170K. The absorption spectrum in (a) shows the Fe^{2+} d to d on-site electronic transitions at ~1.60 and 2.40 eV, respectively. The observed electro-optical effects are stronger around the rising slope of the 1.60 eV peak and vary from +4% to -5% at 78K, and from +3.5 to -1.5% at 170K, respectively. The inset in (b) shows the electro-optical signal as a function of applied voltage at 78 and 170K.²⁵

Conclusion

Much effort has been made in fabricating film of $R\text{Fe}_2\text{O}_4$, which is the candidate of electronic ferroelectric. In this paper, the film growth and electric, magnetic and optical properties of the films are briefly reviewed. Although these research has short history, the charge order was directly observed just recently. Also some data indicate the spin-charge-orbital coupling. The research on the optical property progressed. Attractive properties for application are also reported. The spin-charge-orbital coupling and magnetic memory effect

can be applied to novel memory devices. The nonlinear electric conductivity can be applied to switching devices.

Furthermore, physical investigation and engineering started recently, taking advantage of the film. J. A. Mundy et al. fabricated superlattice of LuFe_2O_4 and LuFeO_3 recently.³³ Such investigation characteristic of film will be activated.

Acknowledgment

None.

Author contribution

None.

References

- Kimizuka N, Takayama-Muromachi E, Siratori K. Handbook on the Physics and Chemistry of Rare Earths. In: Gschneidner KA, Eyring L, editors. North-holland, Elsevier. 1990;13:283–384.
- Yamada Y, Nohdo S, Ikeda N. Incommensurate charge ordering in charge-frustrated LuFe_2O_4 system. *J Phys Soc Jpn*. 1997;66(12):3733–3736.
- Ishihara S. Electronic Ferroelectricity and Frustration. *J Phys Soc Jpn*. 2010;79(1):011010.
- Ikeda N. Ferroelectricity from iron valence ordering in the charge-frustrated system LuFe_2O_4 . *Nature*. 2005;436(7054):1136–1138.
- Ikeda N. Electric Field Response of Stoichiometric LuFe_2O_4 . *Ferroelectrics*. 2011;414:41–47.
- Angst M. Charge Order in LuFe_2O_4 : Antiferroelectric Ground State and Coupling to Magnetism. *Phys Rev Lett*. 2008;101(22):227601.
- De Groot J. Charge Order in LuFe_2O_4 : An Unlikely Route to Ferroelectricity. *Phys Rev Lett*. 2012; 108(18):187601.
- Nagata T. Electric spontaneous polarization in YbFe_2O_4 . *Appl Phys Lett*. 2017;110(5):052901.
- Portengen T, Oestreich T, Sham LJ, et al. Theory of electronic ferroelectricity. *Phys Rev B*. 1996;54:17452.
- Tanaka M. Ferrites Proc 3rd Int Conf on Ferrites Kyoto; 1980.
- Itoh H. Ultrafast melting of charge ordering in LuFe_2O_4 probed by terahertz spectroscopy. *Journal of Luminescence*. 2013;133:149–151.
- Nagata T. Nonlinear Electric Conductivity of Charge Ordered System RFe_2O_4 ($R=\text{Lu}, \text{Yb}$). *Ferroelectrics*. 2013;442(1):45–49.
- Siratori K, Funahashi S, Iida J, et al. Proc. 6th Int Conf Ferrites, 703. Tokyo and Kyoto; 1992.
- Kambe T. Magnetoelectric Effect Driven by Magnetic Domain Modification in LuFe_2O_4 . *Phys Rev Lett*. 2013;110(11):117602.
- Michiuchi T. Stoichiometric Study of the Dielectric and Magnetic Properties in Charge Frustrated System LuFe_2O_4 . *Ferroelectrics*. 2009;378:175–180.
- Fujiwara K. Possible charge order structure of stoichiometric YbFe_2O_4 . *Ferroelectrics*. 2017;512(1):85–91.
- Seki M. Growth of epitaxial TmFeCuO_4 thin films by pulsed laser deposition. *Journal of Crystal Growth*. 2010;312:2273–2278.
- Liu J, Wang Y, Dai JY, et al. Structural and dielectric properties of LuFe_2O_4 thin films grown by pulsed-laser deposition. *Thin Solid Films*. 2010;518:6909–6914.
- Rai RC, Delmont A, Sprow A, et al. Spin-charge-orbital coupling in multiferroic LuFe_2O_4 thin films. *Appl Phys Lett*. 2012;100(21):212904.
- Wang W. Growth diagram and magnetic properties of hexagonal LuFe_2O_4 thin films. *Phys Rev B*. 2012;85:155411.
- Zeng M. Dielectric tunability and magnetoelectric coupling in LuFe_2O_4 epitaxial thin film deposited by pulsed-laser deposition. *Thin Solid Films*. 2012;520(20):6446–6449.
- Mundy JA, Mao Q, Brooks CM, et al. Atomic-resolution chemical imaging of oxygen local bonding environments by electron energy loss spectroscopy. *Appl Phys Lett*. 2012;101:042907.
- Brooks CM. The adsorption-controlled growth of LuFe_2O_4 by molecular-beam epitaxy. *Appl Phys Lett*. 2012;101:132907.
- Fujiwara K, Hori T, Tanaka H, et al. Electric-field breakdown of the insulating charge-ordered state in LuFe_2O_4 thin films. *J Phys D: Appl Phys*. 2013;46:155108.
- Cai B, Nakarmi ML, Franks BS, et al. Electro-optical effects and temperature-dependent electrical properties of LuFe_2O_4 thin films. *Thin Solid Films*. 2014;562:490–494.
- Rai RC. Signature of structural distortion in optical spectra of YFe_2O_4 thin film. *Aip Advances*. 2016;6(2):025021.
- Kashimoto R, Yoshimura T, Ashida A, et al. (2016) Lowering the growth temperature of strongly-correlated YbFe_2O_4 thin films prepared by pulsed laser deposition. *Thin Solid Films*. 614:44–46.
- Fujii T. Growth and charge ordering of epitaxial YbFe_2O_4 films on sapphire using Fe_3O_4 buffer layer. *Japanese Journal of Applied Physics*. 2018;57:010305.
- Seki M, Konya T, Inaba K, et al. Epitaxial Thin Films of InFe_2O_4 and InFeO_3 with Two-Dimensional Triangular Lattice Structures Grown by Pulsed Laser Deposition. *Applied Physics Express*. 2010;3:105801.
- Fujiwara K. Iron vacancy effect on the magnetization of YbFe_2O_4 . *Trans Mat Res Soc Japan*. 2016; 41(1):139–142.
- Nagata T. Control of Fermi Level by Variation of Charge Ordering State in $\text{Yb}_{1-x}\text{Ti}_x\text{Fe}_2\text{O}_4$. *Trans Mater Res Soc Jpn*. 2016;41(3):269–271.
- Xiang HJ, Whangbo MH. Charge Order and the Origin of Giant Magnetocapacitance in LuFe_2O_4 . *Phys Rev Lett*. 2007;98(24):246403.
- Mundy JA. Atomically engineered ferroic layers yield a roomtemperature magnetoelectric multiferroic. *Nature*. 2016;537:523–527.